Vibration-based damage alarming criteria for wind turbine towers

Cong-Uy Nguyen[a], Thanh-Canh Huynh[b], Ngoc-Loi Dang[c] and Jeong-Tae Kim[*]

Department of Ocean Engineering, Pukyong National University,
599-1 Daeyon-3dong, Nam-gu, Busan 608-737, Republic of Korea

Abstract. In this study, the feasibility of vibration-based damage alarming algorithms are numerically evaluated for wind turbine tower structures which are subjected to harmonic force excitation. Firstly, the algorithm of vibration-based damage alarming for the wind turbine tower (WTT) is visited. The natural frequency change, modal assurance criterion (MAC) and frequency-response-ratio assurance criterion (FRRAC) are utilized to recognize changes in dynamic characteristics due to a structural damage. Secondly, a finite element model based on a real wind turbine tower is established in a structural analysis program, Midas FEA. The harmonic force is applied at the rotor level as presence of excitation. Several structural damage scenarios are numerically simulated in segmental joints of the wind turbine model. Finally, the natural frequency change, MAC and FRRAC algorithm are employed to identify the structural damage occurred in the finite element model. The results show that these criteria could be used as promising damage existence indicators for the damage alarming in wind turbine supporting structures.

Keywords: wind turbine tower; vibration-based damage alarming; harmonic force excitation; modal parameters; modal assurance criterion; frequency-response-ratio assurance criterion

1. Introduction

In the recent years, wind energy has been receiving significant attention of many governments since the renewable wind energy produces no greenhouse gas, which is a main cause of global warming. In Europe, with a total installed capacity of 153.7 GW, the wind energy now overtakes coal as the second largest form of power generation capacity in 2016. It is reported that electricity generation from wind energy covers 10.4 % of the EU-28 total electricity demand (Pineda *et al*. 2016). In order to fulfill clean energy demand, more wind turbine towers will be installed in the coming years. The strong investment into the wind energy harvest leads to consideration of safety and durability of wind turbine towers. During their lifetime, the slender vertical wind tower exposes to strong winds frequently that can lead to large vibration and repeated stress cycles causing damage in structure (Benedetti *et al*. 2011). Therefore, the wind turbine towers should be monitored and

---

[*]Corresponding author, Professor, E-mail: idis@pknu.ac.kr
[a] Graduate Student, E-mail: uyznob@gmail.com
[b] Post-Doctoral Researcher., E-mail: ce.huynh@gmail.com
[c] Graduate Student, E-mail: loi.ngocdang@gmail.com

maintained to ensure the safety as well as integrity of the system.

It is well-known that the structural damage causes a change of structural parameters such as mass, stiffness and damping. Consequently, it alters the dynamic responses of the system such as acceleration and modal parameters (Pandey *et al.* 1994). In the past, there were considerable efforts in vibration-based structural health monitoring which utilized dynamic measurements to extract damage-sensitive features (You *et al*. 2013, Kim *et al*. 2014, Kim *et al*. 2016). Many researchers employed the change in natural frequencies to detect structural damages (Vandiver 1977, Farrar *et al.* 1994). Some researches considered mode shape changes as indication of damages in structure (Kim *et al.* 1995, Kim *et al.* 2003). There were other studies on mode shape curvature, flexibility, stiffness matrix (Doebling *et al.* 1998). However, there have been only a few studies conducted on the wind turbine tower using vibration-based structural health monitoring. Benedetti *et al.* (2011) examined strain response of wind turbine tower for undamaged and damaged condition. Nguyen *et al.* (2015) attempted to detect damage in a numerical model of a wind turbine structure by using the frequency-based and mode shape-based damage detection methods. Nguyen *et al.* (2017) employed a hybrid impedance and vibration-based algorithms for the damage detection in a lab-scaled wind turbine tower model. Despite of their attempts, there exists a need to simulate dynamic behavior of the real-scaled wind turbine structures under a real operation condition such as wind force excitation. There is also a need to comparatively examine the sensitivity of damage indicators for an establishment of the real-time health monitoring system of wind turbine structures in practices.

This study has been motivated to numerically verify the vibration-based structural damage alarming criteria for wind turbine towers which are subjected to harmonic force excitation. Firstly, the algorithm of vibration-based damage alarming for the wind turbine tower is visited. The natural frequency change, MAC and FRRAC are utilized to recognize changes in dynamic characteristics due to the structural damage. Secondly, the finite element model based on a real wind turbine tower is established in a structural analysis program, Midas FEA. The harmonic force is applied at the rotor level as the presence of excitation. Several structural damage scenarios are numerically simulated in segmental joints of the wind turbine tower model. Finally, the natural frequency change, MAC and FRRAC indices are employed to identify the structural damage occurred in the finite element model. The results show that these indices could be used as promising damage indicators for the damage alarming in the wind turbine tower.

2. Vibration-based damage alarming for wind turbine tower

2.1 Vibration-based damage alarming algorithm for wind turbine tower

The vibration-based damage alarming algorithm is developed for wind tower (WTT) supporting structures via using the natural frequency change, MAC and FRRAC. These indices are known as sensitive indicators with the change of structural parameters such as mass, stiffness and damping so they are investigated to detect damage occurrence through in WTT model. In addition, the selected indicators can be embedded in a real-time system for field application since they require only simple and quick computation. The process of proposed algorithm includes 4 steps as illustrated in Fig. 1. In step 1, acceleration signals from sensors, which are equipped along the wind turbine supporting structure, are recorded during the operation. In step 2, the natural frequencies and mode shapes are extracted via the frequency domain decomposition method, as described in Section 2.2. The natural frequency change, MAC and FRRAC are computed to evaluate the damage occurrence in the wind
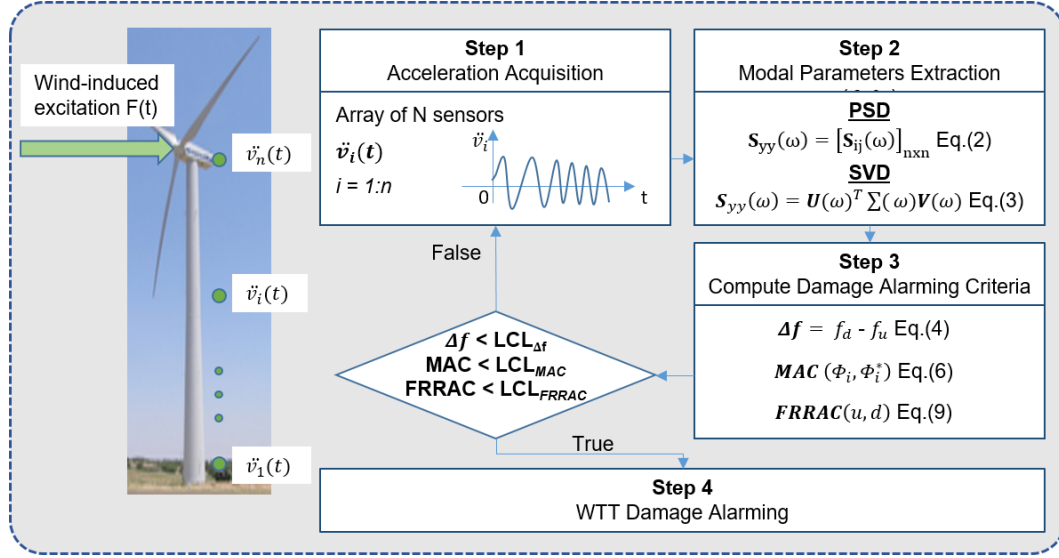
Fig. 1 Vibration-based damage alarming algorithm

turbine supporting structure in step 3. If there is existence of damage, the natural frequency change, MAC and FRRAC values will be lower than a lower control limit. Subsequently, an alarm of damage existence in WTT is raised in step 4. Otherwise, the loop continues if those conditions are not satisfied. In short, the quick evaluation of structural condition is processed by acquiring and analyzing acceleration signal from an array of sensors in a predefined period.

2.2 Modal parameters identification method

Provided that the structure has *NE* elements and *N* nodes. By assuming that the structure behaves linearly, the acceleration response vector at a certain time *t* for a multi-degree of freedom system can be written as

$$\{\ddot{V}(t)\} = [M]^{-1}(\{F(t)\} - [C]\{\dot{V}(t)\} - [K]\{V(t)\})$$ (1)

in which $[M]$, $[C]$ and $[K]$ are mass, damping and stiffness matrix of the system. $\{V\}$, $\{\dot{V}\}$, $\{\ddot{V}\}$ are the displacement, velocity and acceleration response vectors. As described in Eq. (1), the acceleration response at any location $(\ddot{v}_1(t), \ddot{v}_i(t) \ldots \ddot{v}_n(t))$ contains the information of structure $([M], [C]$ and $[K])$. From these vibration responses, the modal analysis can be performed in time-domain or frequency-domain to extract modal parameters. As the frequency-domain method, frequency domain decomposition (FDD) method is fast and accurate compared to other methods. Therefore, it is broadly used for experimental modal analysis. The FDD method utilizes the singular value decomposition of the power spectral density (PSD) matrix (Brinker *et al.* 2000, Yi and Yun 2004). The PSD matrix $\boldsymbol{S}_{yy}(\omega)$ can be constructed by cross-spectrums for all measured accelerations as

$$\boldsymbol{S}_{yy}(\omega) = [\boldsymbol{S}_{ij}(\omega)]_{n \times n}$$ (2)

where *n* is the number of sensors. Then the PSD matrix is decomposed by using singular value decomposition (SVD) algorithm as

$$S_{yy}(\omega) = U(\omega)^T \Sigma(\omega) V(\omega) \qquad (3)$$

where $\Sigma(\omega)$ is a diagonal matrix containing the singular values $\sigma_i(\omega)\,(i=1,...,n)$ of its PSD matrix, $U(\omega)$ and $V(\omega)$ are unitary matrices. $U(\omega)$ is equal to $V(\omega)$ since $S_{yy}(\omega)$ is symmetric. When peak frequencies in the first singular values $\sigma_i(\omega)$ are found, the mode shapes are extracted from any of column vectors of $U(\omega_m)$ at the corresponding peak frequencies. The natural frequencies and mode shapes, which are extracted from the FDD method, are prepared for the damage alarming criterions as in following section.

2.3 Damage alarming criteria

2.3.1 Natural frequency change
The equation of natural frequency change is written as

$$\Delta f = f_d - f_u \qquad (4)$$

in which the f_u, f_d are the natural frequency of undamaged baseline and damaged structure. Basically the structural stiffness is reduced due to the damage existence. Then the frequency change is equal to 0 if no damage occurs and smaller than 0 if damage occurs. However, due to experimental and environmental errors, the frequency change may be smaller than 0 although damage does not occur. To deal with the uncertain conditions (Huynh *et al.* 2014), the lower control limit of the natural frequency change (LCL$_{\Delta f}$) is adopted for alarming damage occurrence as follows

$$LCL_{\Delta f} = \mu_{\Delta f} - 3\sigma_{\Delta f} \qquad (5)$$

where $\mu_{\Delta f}$ and $\sigma_{\Delta f}$ are mean and standard deviation of the frequency change at undamaged condition, respectively.

2.3.2 Modal assurance criterion
In vibration-based method, the modal assurance criterion (MAC) is popular for quantitative comparison of modal vectors. The MAC measures the level of linear correlation between two modal parameters before and after the occurrence of damage (West 1984). The variation of mode shape vectors between each damage scenario and intact one is examined by modal assurance criterion as

$$MAC\,(\Phi_i, \Phi_i^*) = \frac{[\Phi_i^T \Phi_i^*]^2}{\left[\Phi_i^T \Phi_i\right]\left[\Phi_i^{*T} \Phi_i^*\right]} \qquad (6)$$

where Φ_i, Φ_i^* are the Eigen vectors in mode *i* of intact and damage scenarios respectively. If the structure stays intact, the MAC will be unity. While it is lower than unity according to damage existence. To deal with the uncertain conditions that can be caused by experimental and environmental errors, the lower control limit of the MAC (LCL$_{MAC}$) is adopted for alarming damage occurrence as follows

$$LCL_{MAC} = \mu_{MAC} - 3\sigma_{MAC} \qquad (7)$$

where μ_{MAC} and σ_{MAC} signify mean and standard deviation of the MAC at undamaged condition, respectively.

2.3.3 Frequency-response-ratio assurance criterion

As shown in Eq. (1), with the known force vector $\{F(t)\}$, change in acceleration signals can represent of damage occurrence. However, the external excitation is usually not determined in field practices. Therefore, the frequency-response-ratio assurance criterion (FRRAC) is selected as a damage indicator because it can eliminate the effect of external force. The *FRRAC* is computed simply by using two acceleration data measured from two different sensors (Kim *et al.* 2010). The frequency response ratio between signals from location i and $i+1$ is defined as

$$FRR_{i,i+1}(\omega) = \frac{S_{i+1,i}(\omega)}{S_{i+1,i+1}(\omega)} \tag{8}$$

where $S_{i+1,i}(\omega)$ and $S_{i+1,i+1}(\omega)$ are cross-spectral density (CSD) and auto-spectral density (ASD) functions respectively. By comparing a frequency-response-ratio measured at an undamaged baseline state to the corresponding one at subsequent damaged state, the *FRRAC* is defined, as follows

$$FRRAC(u,d) = \frac{[FRR_u^T.FRR_d^T]^2}{[FRR_u^T.FRR_u][FRR_d^T.FRR_d]} \tag{9}$$

where the subscript u and d denote the undamaged state and corresponding damaged state. This equation represents the linear relationship between the undamaged frequency-response-ratio (*FRR_u)* and damage frequency-response ratio (*FRR_d)*. The *FRRAC* is always unity if the structure is intact. Otherwise, it gets lower than unity with respect to damage occurrence. The relative change of *FRRAC* is computed from Eq. (9) and the $FRRAC_{u,u}$ is always unity while the $FRRAC_{u,d}$ is under unity with damaged condition.

$$\Delta FRRAC = \frac{|FRRAC_{u,d} - FRRAC_{u,u}|}{FRRAC_{u,u}} \times 100\% \tag{10}$$

To avoid uncertainties caused by experimental and environmental errors, the lower control limit of the FRRAC (LCL_FRRAC) is adopted for alarming damage occurrence as follows

$$LCL_{\mathrm{FRRAC}} = \mu_{\mathrm{FRRAC}} - 3\sigma_{\mathrm{FRRAC}} \tag{11}$$

where μ_{FRRAC} and σ_{FRRAC} are mean and standard deviation of the FRRAC at undamaged condition, respectively.

3. Finite element analysis of wind turbine model

3.1 Description of finite element model

The finite element model is based on a real WTT, which is located in Hankyung II Wind Park, Jeju Island, Korea. The type of WTT is V90-3.0 MW with nominal rating 3000 kW. The cut-in wind speed is 4 m/s while the cut-out and 25 m/s. There are three blades up wind direction. Nacelle and Rotor weighs 68 and 39.8 tons respectively. The real structure is 80 m high including a hub.

There are four main segments in the tower. Each main segment has a flange at two tips so each one combines together through bolt connections. The first segment is embedded in the foundation and only 0.55 m is above the foundation surface. The second segment is 19.21 m long while the two remaining segments are around 29 m, as shown in Fig. 2. Each main segment is formed by several

sections with thickness changing along elevation. The Table 1 lists the variation of section's thickness with respect to the increasing height.

The tubular tower material is S355 J2G31 with 2% damping ratio. The top level diameter is 2.316 m and the bottom level is 4.15 m. The finite model is established by a commercial structural program, MIDAS FEM as in Fig. 2. As shown in Fig. 2(a), the tower is modeled by shell elements with thickness varying from 40 mm to 16 mm as real design. At any section, there are always 36 divisions along perimeter. The height of shell elements is five times its width. On the top of model, the rotor and nacelle are simulated as independent lump masses. These masses are linked rigidly to the top flange of wind turbine tower. All degree-of-freedoms of the bottom of WTT model are constrained.

For the transient analysis, a harmonic force is applied at the rotor location as shown in Fig. 2(b). The excitation acts along the wind direction, which is the X direction in FEM model. The function of force is $F = 10sin(40\pi t)$ (kN). The amplitude of the force is determined based on wind speed following the ASCE Standard (ASCE 2002). The operational wind speed range of the wind turbine structure is 0 to 25 m/s. In this study, wind speed is selected as 8.5 m/s. To extract the vibration responses (i.e., acceleration signal) of WTT under harmonic force excitation, ten points are selected as Fig. 2(b). The elevation and location are listed in Table 2. The sensor location includes flange connections which are important locations to structural conditions. It is assumed that the sensors are equipped along the interior of tower. In the extraction of acceleration signal, the sampling frequency is 50 Hz and the sampling duration is 660 s.
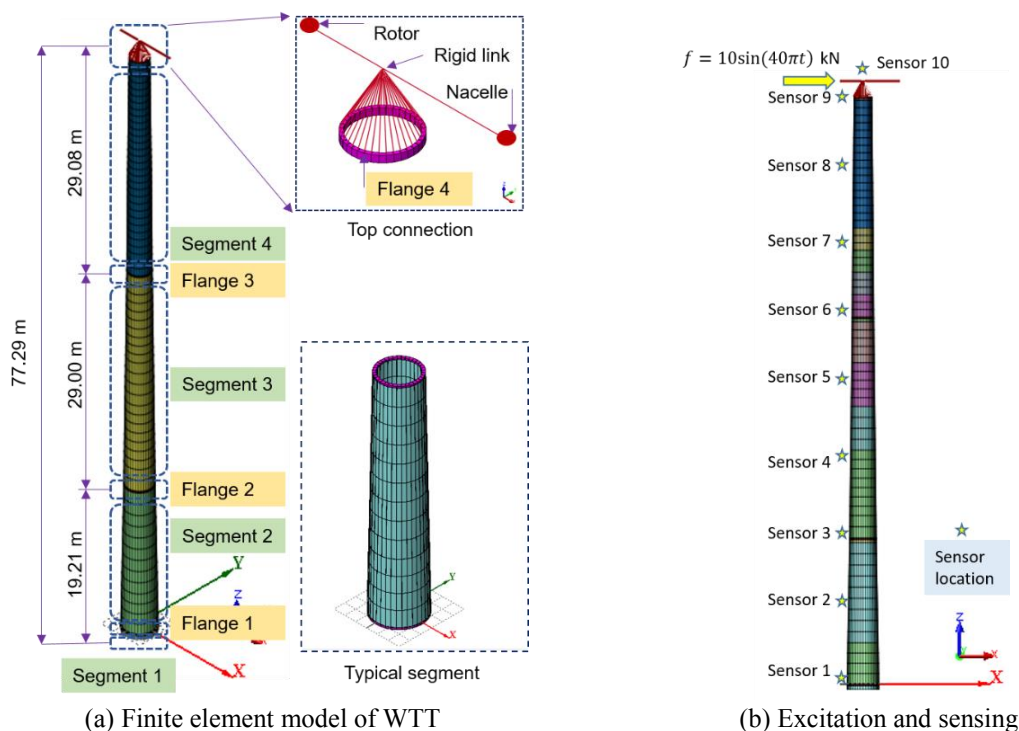

(a) Finite element model of WTT   (b) Excitation and sensing

Fig. 2 Finite element model of WTT model

Table 1 Cross-sectional thickness of WTT model

Elevation (m)	Thickness (mm)
0 ÷ 5.4	40
5.4 ÷ 21.9	26
21.9 ÷ 30.6	24
30.6 ÷ 36.4	23
36.4 ÷ 42.2	22
42.2 ÷ 50.9	21
50.9 ÷ 53.8	19
53.8 ÷ 56.7	18
56.7 ÷ 59.6	17
59.6 ÷77.3	16

Table 2 Sensor location on WTT model

Sensor ID	Location	Elevation (m)
S1	Flange 1	0.55
S2	-	10.5
S3	Flange 2	19.76
S4	-	30.17
S5	-	40.58
S6	Flange 3	48.77
S7	-	58.62
S8	-	68.46
S9	Flange 4	77.85
S10	Hub	78.93

The eigenvalue analysis is implemented to achieve the modal characteristics of the WTT model. Four Eigen modes were found in 0-10 Hz. Fig. 3 shows natural frequencies and mode shapes along the X direction. Natural frequencies of four modes are 0.3115 Hz, 2.2580 Hz, 5.4126 Hz, and 9.7851 Hz, respectively. The extracted mode shapes are bending motions. It is noted that the rotor and nacelle axis are always perpendicular to the tower in every mode due to the rigid link model.
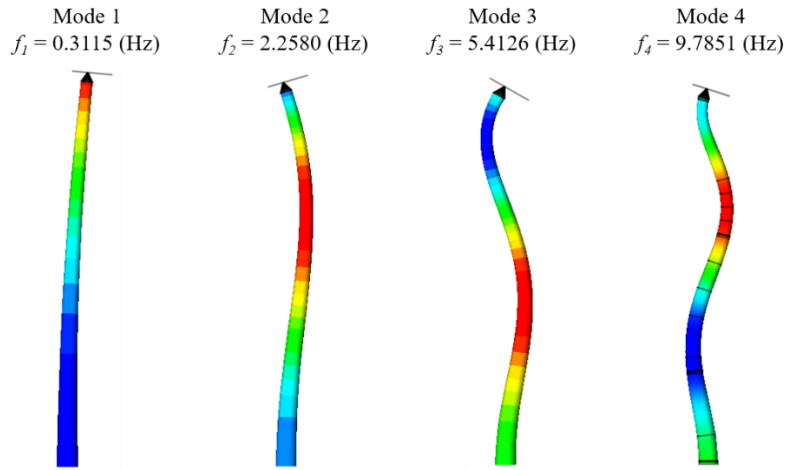
Fig. 3 Mode shapes in X direction of WTT model

3.2 Simulation of harmonic force excitation

The model is excited by the harmonic force at the rotor location. The excitation acts along the wind direction, which is the X direction in FEM model. The acceleration signals along wind are recorded from each sensor on the tower. The acceleration signals are extracted from the time history analysis of the finite element model.

The acceleration signals from the flanges (i.e., S1, S3, S6 and S9) are plotted as in Fig. 4. The maximum amplitudes of the acceleration responses at S1 and S3 are 1.05×10^{-5} g and 1.06×10^{-3} g, respectively. The maximum amplitudes of the acceleration responses at S6 and S9 are 1.57×10^{-3} g and 7.98×10^{-3} g, respectively. The amplitude of the acceleration signals increases along with the elevation of the sensor. The phase of the acceleration signal is slightly different according to the elevation of the sensors.

4. Numerical verification of vibration-based damage alarming algorithm for wind turbine tower

4.1 Structural damage scenarios

Four structural damage scenarios are investigated as shown in Table 3. The damage locations are assumed in connections between consecutive segments of the tower. These segmental joints are vulnerable during operation under wind load. The damage is simulated as the percentage of reduction in the elastic modulus. In case 1, the first flange is simulated with 25% reduction in the stiffness.

The same assumption is in case 4 with only single damage location. Multi-damage investigation is in case 2 and 3 where severe damage occurs simultaneously at two random flanges. 20% reduction in the elastic modulus is the percentage of damage severity of two simultaneous flanges which are examined in this analysis.
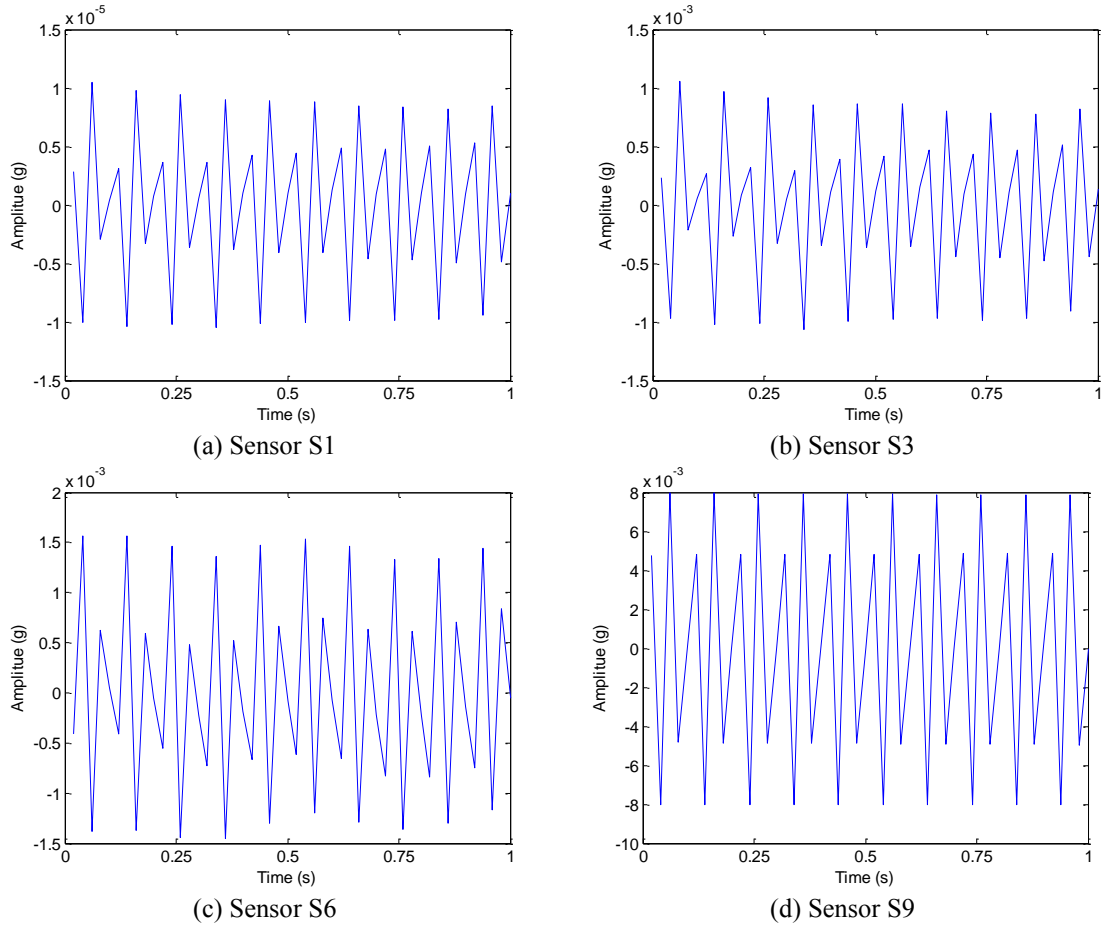
(a) Sensor S1   (b) Sensor S3

(c) Sensor S6   (d) Sensor S9

Fig. 4 Acceleration signals of WTT model

Table 3 Structural damage scenarios of WTT model

Damage case	Damage simulation		
	Location	Elevation (m)	Severity
Intact	-	-	-
1	Flange 1	0.55	25%
2	Flange 1 and 3	0.55 and 48.77	20% and 20%
3	Flange 2 and 4	19.76 and 77.85	20% and 20%
4	Flange 4	77.85	25%

4.2 Identification of modal parameters

As described in Fig. 1, the modal parameters of the WTT model are extracted by the FDD method from the acceleration signal. In the FDD method, the PSD is calculated by Eq. (2) and the singular values are calculated by Eq. (3). It is known that the identification of higher modes based on FDD is relatively unstable. To enhance the accuracy for the identification of such higher modes, the sampling frequency and the number of FFT (Fast Fourier Transform) should be selected appropriately. In this study, the number of FFT is selected as 2^{15} and the FFT number is selected as 50 Hz. As the result, the resolution of frequency is 0.0015 Hz, which is smaller than the changes of natural frequencies for investigated damage cases in the WTT. Fig. 5 shows the singular value of the acceleration signal for the intact WTT model. In the figure, peaks indicate vibration modes of WTT for the harmonic excitation. It is clear that there are four peaks which indicate first four modes along X direction respectively. Four modes are extracted at 0.3113 Hz, 2.2583 Hz, 5.4092 Hz and 9.7931 Hz, respectively. The extracted modal parameters of the intact model including the mode shape and natural frequency are similar to the eigenvalue analysis. The mode shapes are extracted from the singular value and the unitary matrix as shown in Fig. 6. The mode shapes extracted from the FDD method are coincident with those of the eigenvalue analysis results (see Fig. 3).
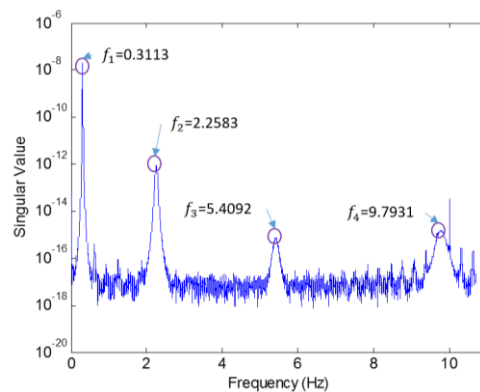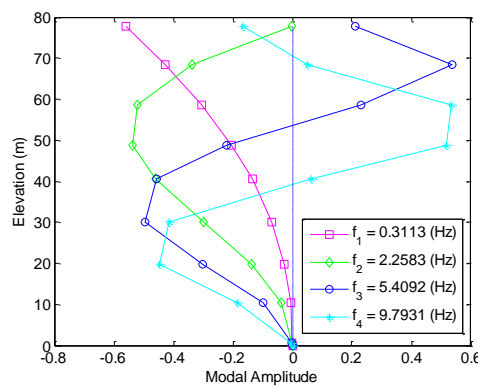

Fig. 5 Singular value of intact WTT model

Fig. 6 Mode shapes of intact WTT model

(a) 1st peak: 0.303-0.319 Hz

(b) 2nd peak: 2.22 – 2.29 Hz

(c) 3rd peak: 5.29-5.53 Hz
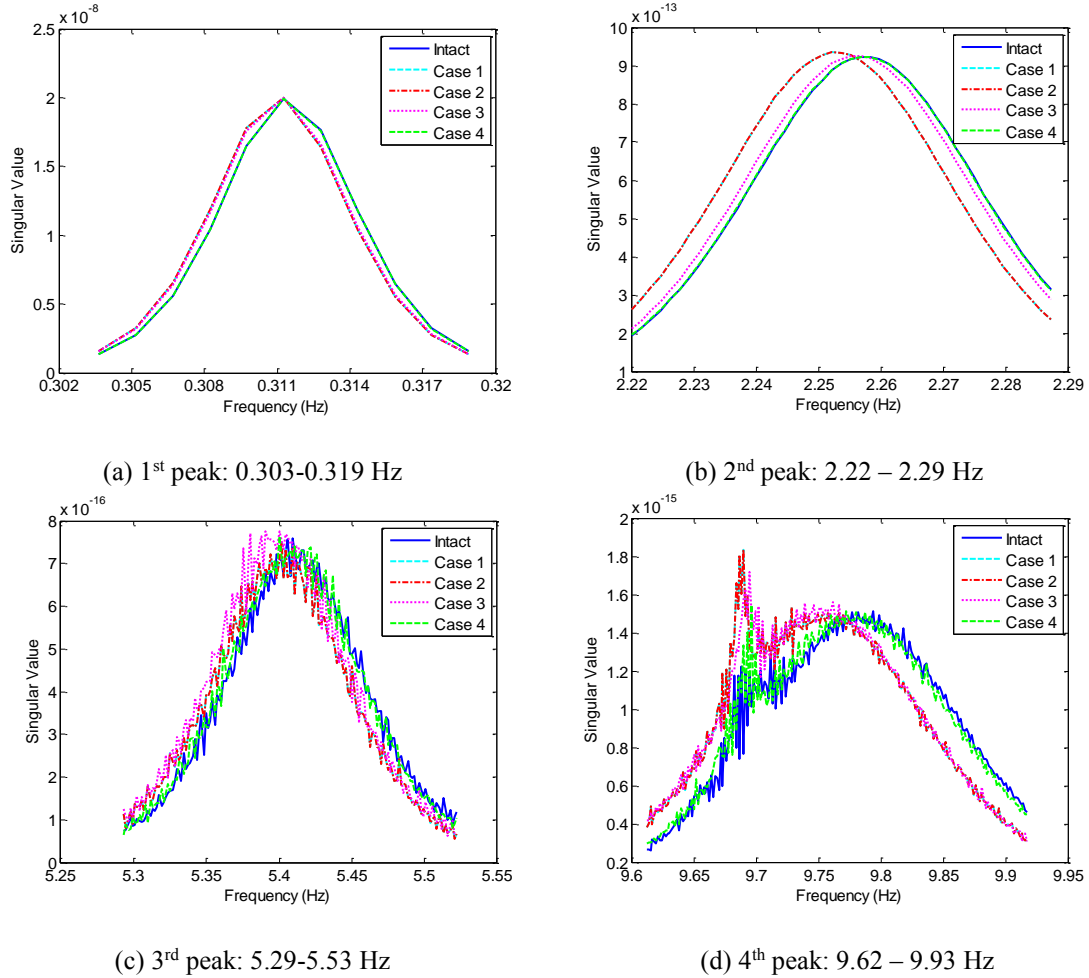
(d) 4th peak: 9.62 – 9.93 Hz

Fig. 7 Change in resonant frequencies of singular values due to damage

The modal parameters of WTT model for the damaged cases are extracted by the same way of intact case. The singular values of each damaged cases are compared to the intact in the Fig. 7. Due to the damage existence, the peaks in singular values shift to the left with respect to the intact one. The shifts get larger for higher modes compared to lower ones.

4.3 Damage alarming

4.3.1 Natural frequency change

The natural frequencies of all damage scenarios are illustrated in Table 4. In the table, the damage alarming criteria Δf of natural frequency are also listed. It is clear that natural frequency decreases when damage occurs in WTT. As the results, most Δf values are negative. The natural frequency reduction increases with respect to a higher mode. It is noted that the natural frequency change is

successful to detect damage occurrence. The first natural frequency does not change in every case.

It seems that the sensitivity of the first mode is relatively small for the flange damage type. The amount of variation of the natural frequencies due to damage is quantified from the absolute value of the ratio between f_u and Δf, as shown in Fig. 8. Relative changes in natural frequencies show the sensitivity of each mode. In the results, mode 4 is the most sensitive to the damage in connection of the flange.

4.3.2 Modal assurance criterion

The mode shapes are extracted from the FDD method. The mode shapes for the damage cases are compared to the intact case in Fig. 9. In the figure, the 1st and 2nd mode shapes are nearly the same in every case while the 3rd and 4th ones change along each scenario. The vertical line stands for the center of static structure. The MAC is computed between intact scenario and each damage one by Eq. (6). The MAC is nearly 1 for mode 1 and mode 2 because there is little change of the 1st and 2nd modes in every case. However, this index decreases larger in mode 3 and mode 4 as presented in Fig. 10. It is noted that the MAC detects damage occurrence with mode 3 and mode 4, successfully.
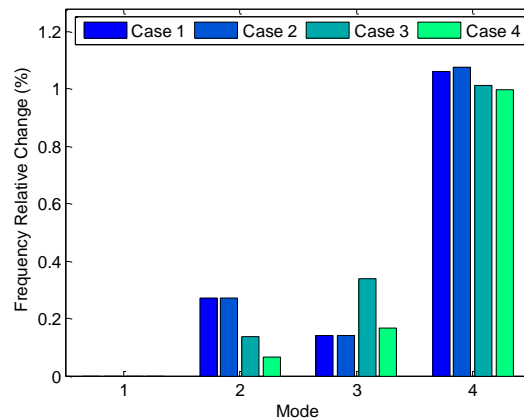

Fig. 8 Relative reduction in natural frequencies due to damage

Table 4 Natural frequencies (Hz) of WTT for all damage cases

Mode	Intact	Case 1		Case 2		Case 3		Case 4	
	f_u	f_d	Δf	f_d	Δf	f_d	Δf	f_d	Δf
1	0.3113	0.3113	0	0.3113	0	0.3113	0	0.3113	0
2	2.2583	2.2522	-0.0061	2.2522	-0.0061	2.2552	-0.0031	2.2568	-0.0015
3	5.4092	5.4016	-0.0076	5.4016	-0.0076	5.3909	-0.0183	5.4001	-0.0091
4	9.7931	9.6893	-0.1038	9.6878	-0.1053	9.6939	-0.0992	9.6954	-0.0977
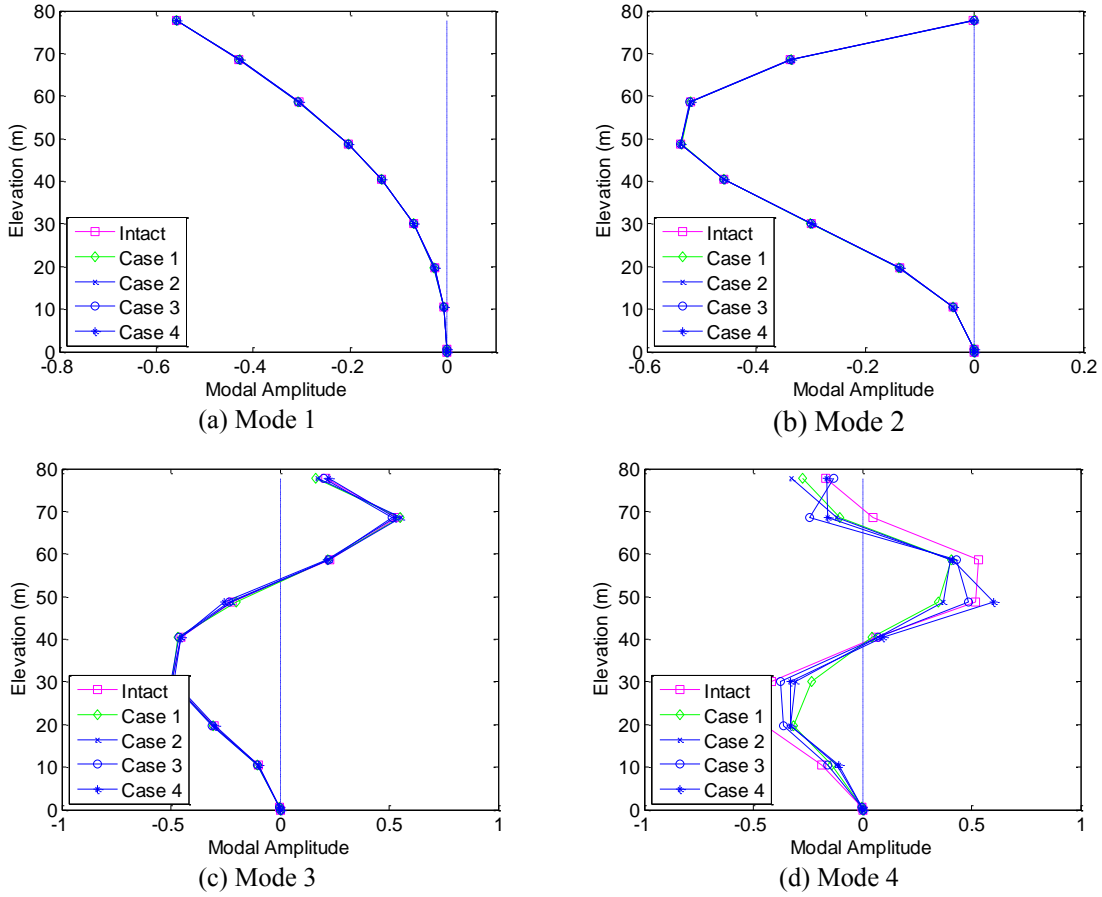
Fig. 9 Mode shapes along X direction of WTT model
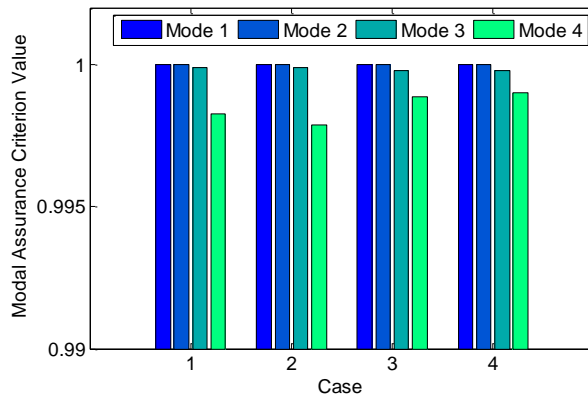
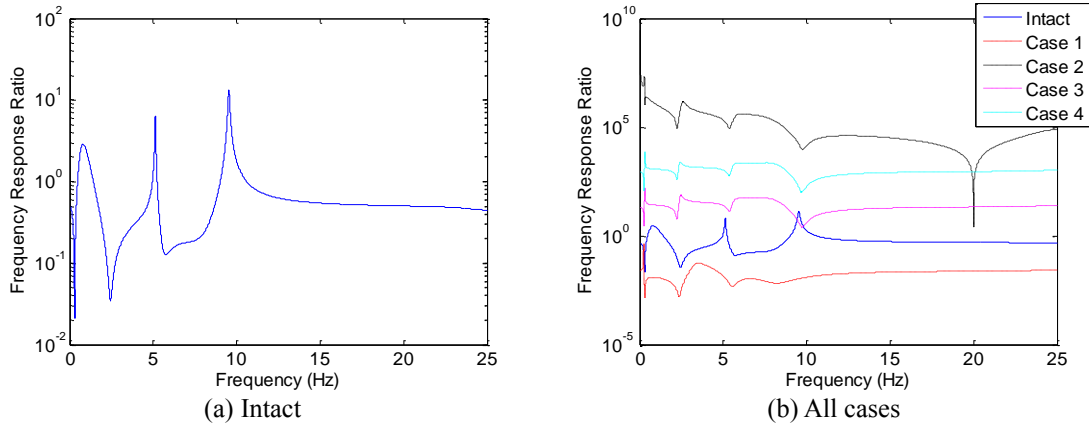Fig. 10 MAC change due to structural damage

(a) Intact   (b) All cases

Fig. 11 FRR from sensor S3 and S6 on WTT model

(a) Case 1   (b) Case 2

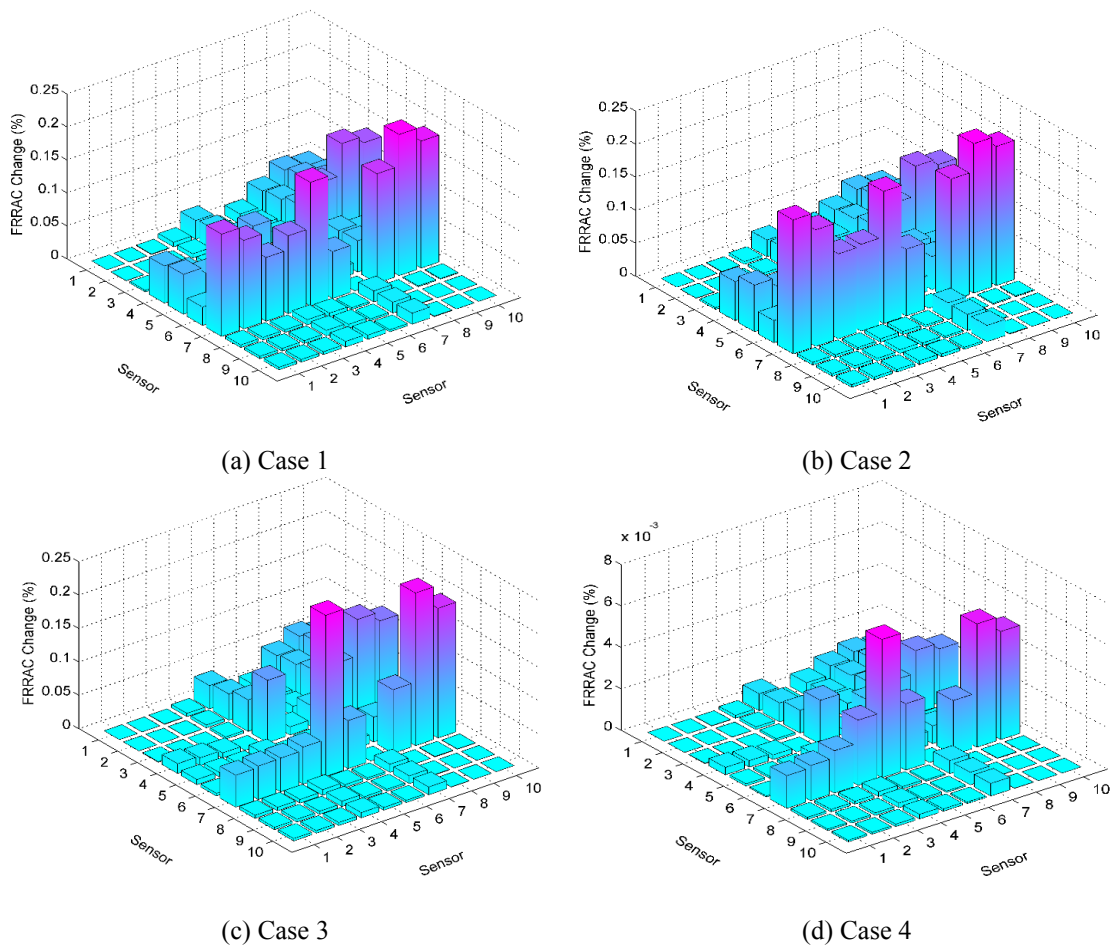(c) Case 3   (d) Case 4

Fig. 12 FRRAC change due to structural damage

4.3.3 Frequency-response-ratio assurance criterion

The acceleration signals from all sensors are utilized to calculate the auto-spectral density (ASD) and cross-spectral density (CSD) from 0 Hz to 25 Hz. Then, the FRR is computed as Eq. (8) and the FRRAC is calculated by Eq. (9). Fig. 11 shows FRR of intact case and damaged cases with sensor S3 and S6. The relative changes of the FRRAC ($\Delta FRRAC$) are calculated by Eq. (10). Fig. 12 shows the relative change of the FRRAC between the intact and damaged cases. The FRRAC criterion succeeds in recognition of damage occurrences in every case. It is noted that the FRRAC from sensor S3 to S7, which are near the damage locations, are more sensitive than those of the remaining sensors.

5. Conclusions

In this study, the vibration-based structural damage alarming for wind turbine tower (WTT) structures subjected to a harmonic force excitation was investigated via numerical finite element analyses. At first, the theory of vibration-based damage alarming algorithm for the WTT was visited. The natural frequency change, MAC and FRRAC were utilized to recognize changes in dynamics features due to structural damage. Then, the finite element model based on a real wind turbine tower was established in a structural analysis program, Midas FEA. The harmonic force was applied at the rotor level as the presence of excitation. Several structural damage scenarios were numerically simulated in segmental joints of the WTT model.

The proposed algorithm could alarm the damage occurrence in the WTT via using the natural frequency change, the MAC and FRRAC indices. Due to the structural damage, the natural frequencies of WTT were reduced larger in high modes as compared to lower ones. Similarly, the MAC was effective at high modes for identification of damage existence. The FRRAC was also successful in recognition of the structural failure from all sensors. For the WTT structure, there are many kinds of damage. Also, from the general information of field experiments, there exist many other causes phenomena (e.g., temperature changes) which affect to the modal characteristics of the structure. As future studies, therefore, it is needed to consider the different damage types and the various experimental conditions for the practicality evaluation of the proposed method.

Acknowledgements

References

Benedetti, M., Fontanari, V. and Zonta, D. (2011), "Structural health monitoring of wind towers: remote damage detection using strain sensors", *Smart Mater. Struct.*, **20**, 1-13.
Brinker, R., Zhang, L. and Andersen, P. (2000), "Modal identification from ambient response using frequency domain decomposition", *Proceeding of the 16th International Modal Analysis Conference*, San Antonio, Texas, USA.

Doebling, S.W., Farrar, C.R. and Prime, M.B. (1998), "A summary review of vibration-based damage identification methods", *J. Sound Vib.*, **30**, 91-105.

Farrar, C.R. (1997), "System identification from ambient vibration measurements on a bridge", *J. Sound Vib.*, **205**(1), 1-18.

Huynh, T.C. and Kim, J.T. (2014), "Impedance-based cable force monitoring in tendon-anchorage using portable PZT-interface technique", *Math. Probl. Eng.*, **2014**, 1-13.

Kim, J.T. and Stubbs, N. (1995), "Model uncertainty and damage detection accuracy in plate-girder bridges", *J. Struct. Eng. - ASCE*, **121**(10), 1409-1417.

Kim, J.T., Huynh, T.C. and Lee, S.Y. (2014), "Wireless structural health monitoring of stay cables under two consecutive typhoons", *Struct. Monit. Maint.*, **1**(1), 047-067

Kim, J.T., Park, J.H., Hong, D.S. and Park, W.S. (2010), "Hybrid health monitoring of prestressed concrete girder bridges by sequential vibration-impedance approaches", *Eng. Struct.*, **32**, 115-12.

Kim, J.T., Ryu, Y.S., Cho H.M. and Stubbs, N. (2003), "Damage identification in beam-type structures: Frequency-based method vs mode-shape-based method", *Eng. Struct.*, **25**, 57-67.

Kim, J.T., Sim, S.H., Cho, S.J. and Yun, C.B. (2016), "Recent R&D activities on structural health monitoring in Korea", *Struct. Monit. Maint.*, **3**(1), 091-114

Nguyen, T.C., Huynh, T.C. and Kim, J.T. (2015), "Numerical evaluation for vibration-based damage detection in wind turbine tower structure", *Wind Struct.*, **21**(6), 657-675.

Nguyen, T.C., Huynh, T.C. and Kim, J.T. (2016), "Hybrid bolt-loosening detection in wind turbine tower structures by vibration and impedance responses", *Wind Struct.*, **24**(4), 385-403.

Pandey, A.K. and Biswas, M. (1994), "Damage detection in structures using changes in flexibility", *J. Sound Vib.*, **169**(1), 3-17.

Pineda, I. and Tardieu, P. (2017), "Wind in power: 2016 European statistics", Wind Europe

Vandiver, J.K. (1977), "Detection of structural failure on fixed platforms by measurement of dynamic response", *J. Petroleum Technol.*, **29**(3), 305:310.

West, W.M. (1984), "Illustration of the use of modal assurance criterion to detect structural changes in an orbiter test specimen", *Proceeding of the Air Force Conference on Aircraft Structural Integrity*, 1-6.

Yi, J.H. and Yun, C.B. (2004), "Comparative study on modal identification methods using output-only information", *Struct. Eng. Mech.*, **17**(3), 445-466.

You, T., Gardoni, P. and Hurlebaus, S. (2013), "Iterative damage index method for structural health monitoring", *Struct. Monit. Maint.*, **1**(1), 89-110.

TY